FRIGID ZONE **MEDICINE**
Original Article • DOI: 10.2478/fzm-2024-0002

Peroxisome proliferator-activated receptors gama ameliorates liver fibrosis in non-alcoholic fatty liver disease by inhibiting TGF-β/Smad signaling activation

Qingwei Zhang[1,2,3], Wenjie Zhao[1,2,3], Zeqi Sun[1,2,3], Xinxin Dong[1,2,3], Liwei Zhu[1,2,3], Zhen Zhang[1,2,3], Ximing Chen[1,2,3], Yingying Hu[1,2,3], Menghan Du[1,2,3], Jiamin Li[2,3,4*], Yong Zhang[1,3,4*]

Abstract

Background: Nonalcoholic fatty liver disease (NAFLD) is a chronic condition characterized by a progressive decline in liver function, leading to disruptions in liver integrity and metabolic function, resulting in lipid deposition and excessive accumulation of extracellular matrix (ECM). The pathogenesis of NAFLD is complex and not yet fully understood, contributing to the absence of specific therapeutic strategies. Peroxisome proliferator-activated receptor gamma (PPARγ) is a ligand-activated transcription factor pivotal in regulating lipid and glucose metabolism. However, the impacts of PPARγ on NAFLD remains insufficiently explored. Thus, this study aimed to investigate the role of PPARγ in NAFLD and its underlying molecular mechanisms. **Methods:** Chemical detection kits were utilized to quantify collagen content, alanine aminotransferase (ALT), and aspartate aminotransferase (AST) level variations. Quantitative real-time polymerase chain reaction (qRT-PCR) was employed to assess alterations in extracellular matrix-related genes and inflammatory response genes in liver tissue and HepG2 cells, while western blotting was conducted to analyze the levels of both PPARγ and the TGF-β/Smad signaling pathway. **Results:** Our findings unveiled significantly reduced PPARγ expression in a rat model of NAFLD, leading to subsequent activation of the TGF-β/Smad signaling pathway. Furthermore, PPARγ activation effectively mitigated NAFLD progression by inhibiting inflammation and fibrosis-related gene expression and collagen production. On a cellular level, PPARγ activation was found to inhibit the expression of extracellular matrix-related genes such as matrix metalloproteinase 2 (MMP2) and matrix metalloproteinase 9 (MMP9), along with inflammatory response genes interleukin (IL)-1β and IL-6. Additionally, PPARγ activation led to a significant decrease in the levels of ALT and AST. At the molecular level, PPARγ notably down-regulated the TGF-β/Smad signaling pathway, which is known to promote liver fibrosis. **Conclusion:** These groundbreaking findings underscore PPARγ activation as a promising therapeutic approach to delay NAFLD progression by targeting the TGF-β/Smad signaling pathway in hepatic cells. This highlights the potential of PPARγ as a promising therapeutic target for NAFLD management in clinical settings.

Keywords

NAFLD; PPARγ; TGF-β/Smad; liver fibrosis

Received 04 January 2024, accepted 06 February 2024

[1]*Department of Pharmacology, College of Pharmacy, and Department of Cardiology, the Second Affiliated Hospital, Harbin Medical University, Harbin 150081, China.*
[2]*Department of Pharmacology, College of Pharmacy, Harbin Medical University, Harbin 150081, China.*
[3]*The State Key Laboratory of Frigid Zone Cardiovascular Diseases (SKLFZCD), and the Key Laboratory of Cardiovascular Medicine Research, Ministry of Education, Harbin 150081, China.*
[4]*Research Unit of Noninfectious Chronic Diseases in Frigid Zone, Chinese Academy of Medical Sciences, 2019RU070, Harbin 150081, China.*

**Corresponding authors Yong Zhang, E-mail: hmuzhangyong@hotmail.com; Jiamin Li, E-mail: lijiamin0616@163.com*

1 Introduction

Non-alcoholic fatty liver disease (NAFLD), one of the most frequent causes of chronic liver disease worldwide across all age groups, persists at a high prevalence and is increasing globally, posing a serious threat to individual health and life, particularly in frigid regions[1-2]. A nationwide multicenter cross-sectional study was conducted in China to explore region-specific rates of NAFLD. The results of multivariate regression analysis revealed that the percentage of NAFLD in Northern China was approximately twice that of Southern China[3]. Additionally, cold exposure has been found to be associated with a higher prevalence of NAFLD; a

population-based study found that the risk of NAFLD increases during the cold season, independently[4]. Cold stress induces significant physiological changes in various tissues, including the liver[5], affecting liver metabolism and influences energy homeostasis, although this effect is complex[6]. Moreover, the incidence and prevalence of NAFLD are positively correlated with diseases that are positively prevalent in cold areas, such as type 2 diabetes, stroke, and ischemic heart disease[2]. Therefore, it is crucial to gain a comprehensive understanding of the pathogenesis of NAFLD, especially for individuals living in colder areas. NAFLD is a common hepatic condition in patients with obesity, diabetes, and hypertension, which can result in non-alcoholic steatohepatitis and fibrosis[7]. In the progression of NAFLD, lipid accumulation in hepatic cells and excessive deposition of extracellular matrix (ECM), mostly type I and III collagens, result in the formation of a scar and subsequently development of liver fibrosis[8]. However, the molecular mechanisms underlying NAFLD are largely unknown. NAFLD formation, inflammatory changes, and fibrogenesis can be triggered by many signaling molecules, of which transforming growth factor-β (TGF-β) may play an important role in the development of the disease by activating the proliferation and collagen production of hepatic stellate cells (HSCs)[9-10]. Hepatocytes are the most abundant cell type in the liver and play an important role in the maintenance of hepatic function. At present, the role of hepatocytes in hepatic fibrosis has been receiving more attention. Studies have shown that damaged hepatocytes have the potential to synthesis and release TGF-β to promote the activation of hepatic stellate cell, leading to the development of hepatic fibrosis during liver diseases[11-13].

Peroxisome proliferator-activated receptors (PPARs) are members of the nuclear receptor superfamily and ligand-activated transcription factors with important functions in the regulation of cellular differentiation, development, metabolism (carbohydrate, lipid, protein), and proliferation, as well as inflammation in various tissues. Among the PPAR isoforms, PPARγ is particularly known for its regulatory role in glucose metabolism and adipogenesis[14-16]. Furthermore, PPARγ has been associated with obesity in individuals with type 2 diabetes mellitus (T2DM); it decreased free fatty acid deposition in the liver by improving insulin sensitivity in the adipose tissue and the skeletal muscle[17-18]. However, the expression and function of PPARγ in hepatocytes remain unclear. Therefore, the objective of this study was to investigate the essential role of PPARγ in the progression of NAFLD and to explore the underlying mechanisms. To this end, we conducted the present study to examine the impact of PPARγ on NAFLD through both *in vivo* and in vitro approaches and further elucidated its underlying mechanisms. Our findings revealed, for the first time, that activation of PPARγ exhibits anti-fibrosis properties, potentially mediated through its regulation of the TGF-β/Smad signaling pathway in NAFLD.

2 Methods

2.1 Animals

Male Wistar rats (180-220 g) were obtained from the Animal Center of the Second Affiliated Hospital of Harbin Medical University (Harbin, China). The rats were housed under standard animal room conditions (temperature of 22 ± 1°C, humidity of 55%-60%). The animals were randomly divided into two groups: the normal-diet (ND) group and the high fat diet (HFD) group. The HFD group was subsequently maintained on diet with HFD for 18 weeks. The diet contained lard (20%), cholesterol (5%), sucrose (5%), glucose (5%), and salt (6%), which were emulsified in 20% Tween 80 and 30% propylene glycol with distilled water to induce NAFLD. Our animal experiments conformed to the recommendations of the Guide for the Care and Use of Laboratory Animals, published by the US National Institutes of Health (NIH Publication no. 85-23, revised 1996) and were approved by the ethics committee of Harbin Medical University (IRB3001722).

2.2 Cell culture

HepG2 were obtained from American Type Culture Collection and cultured in Dulbecco's modified Eagle's medium (Hyclone, Logan, UT, USA) containing 10% fetal bovine serum (Gibco, Waltham, MA, USA). HepG2 were incubated at 37°C in humidified air with 5% CO_2 for 24 h, and subsequently treated with free fatty acid (FFA) (1 mmol/L, palmitic acid [PA], oleic acid [OA]; PA ： OA, 1 ： 2, 48 h). The cells were incubated with PPARγ-specific agonist rosiglitazone (30 μmol/L, 48 h) and PPARγ-specific inhibitor GW9662 (30 μmol/L, 48 h) purchased from Sigma Aldrich, Germany.

2.3 Real-time PCR

Total RNA was extracted from tissues and cells using TRIzol reagent (Invitrogen, CA, USA) according to the manufacturer's protocols[19-20]. cDNA synthesis was performed using the reverse transcription kit (RR047A, Takara, Otsu City, Shiga Prefecture, Japan). The SYBR Green PCR Master Mix Kit (4913914001, Roche, Basel, Switzerland) was used for real-time PCR to obtain relative quantification of RNA, and qRT-PCR was performed on a 7500 FAST real-time PCR system (Applied Biosisytems, Waltham, MA USA). GAPDH was used as an internal control. The sequences of primers used in our study are listed in Table 1.

2.4 Western blot Analysis

Proteins were extracted from rat liver and HepG2 cells for immunoblotting analysis of TGF-β, p-Smad2/3, Smad2/3, Smad7, and PPARγ. Protein content was determined using the BCA

Table 1. The sequences of primers for used for qRT-PCR in this study.

Gene	Forward primer	Reverse primer
PPARγ	ACCACTCCCATTCCTTTG	CACAGACTCGGCACTCG
TGF-β	GCGAGCGAAGCGACGAGGAG	TGGGCGGGATGGCATCAAGGTA
Col-1	CAATGGCACGGCTGTGTGCG	CACTCGCCCTCCCGTCTTTGG
Col-3	TGAATGGTGGTTTTCAGTTCAG	GATCCCATCAGCTTCAGAGACT
MMP2	AGCTTTGATGGCCCCTATCT	GGAGTGACAGGTCCCAGTGT
MMP9	CACTGTAACTGGGGGCAACT	CACTTCTTGTCAGCGTCGAA
IL-1β	CCCTGCAGCTGGAGAGTGTGG	TGTGCTCTGCTTGAGAGGTGCT
IL-6	TTCCTACCCCAACTTCCAATG	ATGAGTTGGATGGTCTTGGTC
TNFα	CCTCTCTCTAATCAGCCCTCTG	GAGGACCTGGGAGTAGATGAG
CTGF	CAGCATGGACGTTCGTCTG	AACCACGGTTTGGTCCTTGG
Timp1	CTTCTGCAATTCCGACCTCGT	ACGCTGGTATAAGGTGGTCTG
GAPDH	AAGAAGGTGGTGAAGCAGGC	TCCACCACCCAGTTGCTGTA

PPARγ, peroxisome proliferator-activated receptor gamma; TGF-β, transforming growth factor beta 1; Col-1, collagen, type I, alpha 1; Col-3, collagen type III alpha 1; MMP2, matrix metallopeptidase 2; MMP9, matrix metallopeptidase 9; IL-1β, interleukin 1 beta; IL-6, interleukin 6; TNFα, tumor necrosis factor-α; CTGF, connective tissue growth factor; Timp1, Tissue inhibitor of metalloproteinases-1; GAPDH, glyceraldehyde-3-phosphate dehydrogenase.

Protein Assay kit (Solarbio, Beijing, China). The protein samples were separated by SDS-PAGE and transferred to nitrocellulose membranes. The membranes were blocked using 5% filtered non-fat milk for 2 h and then incubated with primary antibodies overnight at 4°C[21], including rabbit TGF-β (Cell Signaling Technology, Danvers, MA, USA), rabbit Smad2/3 (Cell Signaling Technology, Danvers, MA), rabbit p-Smad2/3 (Cell Signaling Technology, Danvers, MA), rabbit Smad7 (Santa Cruz Biotechnology, Dallas, Texas, USA), and rabbit PPARγ (Santa Cruz Biotechnology, Dallas, Texas, USA), followed by incubation with a florescence-labeled secondary antibody. GAPDH (Zhongshanjinqiao, Inc., Beijing, China) was used as an internal control.

2.5 Enzyme-linked immunosorbent assay

Serum levels of IL-1β and IL-6 were detected using the rat IL-1β enzyme-linked immunosorbent assay (ELISA) kit and rat IL-6 ELISA kit (Wuhan Boster Biological Technology, Ltd., Wuhan, Hubei, China), respectively.

2.6 Immunofluorescent staining

Immunofluorescent staining was performed as previously described[22]. After appropriate treatment, HepG2 cells and liver tissue slices were fixed with 4% buffered paraformaldehyde in PBS. The samples were incubated in the blocking solution (1% BSA and 0.1% Triton-X in PBS) at room temperature for 2 h. They were then blocked with goat serum and incubated with PPARγ antibody (Santa Cruz Biotechnology, Dallas, Texas, USA) overnight at 4°C. Subsequently, the samples were probed with florescence-labeled secondary antibody, and immunoblotting staining was examined under a confocal laser scanning microscope (FV300, Olympus, Japan).

2.7 Oil red O staining

To view lipid deposition, Oil red O staining was performed using an Oil red O staining kit (Nanjing Jiancheng Biology Engineering Institute, Nanjing, Jiangsu, China) according to the manufacturer's instructions.

2.8 Measurement of collagen content

Collagen conten was measured using a Sircol soluble collagen assay kit (Biocolor Ltd., Carrickfergus, County Antrim, UK). Lysates (100 mL) were stained with 1 mL of Biocolor dye reagent. The unbound dye solution was removed, and 1 mL of the alkali reagent was added. Absorbance at 540 nm was recorded. The collagen content was quantified and normalized to the total protein of each lysate.

2.9 Statistical analysis

The data are presented as mean±SEM. Differences among multiple groups were analyzed using one-away ANOVA, and statistical comparisons between two groups were performed by *t*-test with Turkey multiple-comparisons test (GraphPad Prism version 8.0, GraphPad Software, CA, USA), $P < 0.05$ was considered significant.

3 Results

3.1 Characterization of nonalcoholic fatty liver disease (NAFLD) rats

To investigate liver dysfunction following NAFLD, we developed a rat model of NAFLD induced by HFD. As shown in Fig. 1A, the

NAFLD rats exhibited significant increases in serum triglycerides (TG) (P = 0.0031), total cholesterol (TCH) (P = 0.0198), and low-density lipoprotein (LDL) (P = 0.0020), while high-density lipoprotein (HDL) (P = 0.0257) levels were decreased. Additionally, alanine aminotransferase (ALT) (P < 0.0001) and aspartate aminotransferase (AST) (P < 0.0001) levels were significantly elevated in the NAFLD group (Fig. 1B). Moreover, the NAFLD group showed a marked increase in the levels of inflammatory cytokines interleukin-1β (IL-1β) (P < 0.0001) and interleukin-6 (IL-6) (P = 0.0006) in serum (Fig. S1A, B). Collagen deposition was also found higher in the NAFLD group (P < 0.0001) (Fig. 1C). Histological analysis of liver sections stained with Oil red O in NAFLD rats revealed typical steatohepatitis phenotypes, characterized by a significant increase in lipid content (Fig. 1D). Furthermore, qRT-PCR analysis of liver tissue in NAFLD rats unveiled up-regulation of mRNA expression of type I collagens (Col-1) (P = 0.0003), type III collagens (Col-3) (P < 0.0001), matrix metalloproteinase 2 (MMP2) (P < 0.0001), and matrix metalloproteinase 9 (MMP9) (P = 0.0009) relative to the Control group (Fig. 1E).

3.2 PPARγ plays a significant role in the development of NAFLD, and its activation inhibited collagen production induced by FFA in HepG2 cells

PPARγ is well-known for its critical role in regulating glucose and adipogenesis. To explore the potential role of PPARγ in NAFLD, we examined the expression of PPARγ in hepatic tissue from NAFLD rats. Our results demonstrated a significant decrease in both mRNA and protein levels of PPARγ in NAFLD compared to the Control group (P < 0.0001 and P < 0.0001, respectively) (Fig. 2A, B). Immunofluorescence staining analysis further confirmed the downregulation of PPARγ expression in the NAFLD group (Fig. 2C).

To further investigate the effect of PPARγ in NAFLD, we developed a cell model of NAFLD induced by free fatty acid (FFA). The Oil red O staining assay revealed significantly increased lipid accumulation in HepG2 cells administered with FFA (Fig. S2A). Then, the expression levels of PPARγ in HepG2 Cells treated with rosiglitazone under FFA conditions were assessed. We observed a significant decrease in PPARγ expression in FFA-treated HepG2 Cells (FFA *vs.* Control, P = 0.0162), which was restored by rosiglitazone (Rosiglitazone *vs.* FFA, P = 0.0094) (Fig. 3A). These findings were further confirmed by immunofluorescence assay (Fig. 3B). Next, we examined relevant indicators to verify whether PPARγ activation could improve NAFLD. We observed that ALT and AST concentrations were significantly increased after incubation with FFA (FFA *vs.* Control, P < 0.0001 and P < 0.0001, respectively), which were inhibited by rosiglitazone (a PPARγ agonist) under FFA conditions (Rosiglitazone *vs.* FFA, P = 0.0103 and P = 0.0114, respectively) (Fig. 3C, D). Moreover, activation of PPARγ by rosiglitazone reduced collagen production induced by FFA (FFA *vs.* Control, P < 0.0001; Rosiglitazone *vs.* FFA, P < 0.0001) (Fig. 3E). Furthermore, rosiglitazone restored the up-regulation of Col-1 (FFA *vs.* Control, P = 0.0004; Rosiglitazone *vs.* FFA, P = 0.0002), Col-3 (FFA *vs.* Control, P < 0.0001; Rosiglitazone *vs.* FFA, P = 0.0001), MMP2 (FFA *vs.* Control, P = 0.0015; Rosiglitazone *vs.* FFA, P = 0.0030), and MMP9 (FFA *vs.* Control, P = 0.0147; Rosiglitazone *vs.* FFA, P = 0.0281) mRNA levels in FFA-treated HepG2 cells, suggesting its potential to inhibit collagen-related gene expression and collagen production in hepatocytes after FFA treatment (Fig. 3F-I). Rosiglitazone did not significantly affect the mRNA level of tissue inhibitor of metalloproteinases 1 (Timp1) in hepatocytes (Fig. S3A). In most chronic liver diseases, HSCs are considered the main contributors to fibrosis as they primarily produce collagen. However, studies have shown that hepatocytes, the main cell type in the liver, can activate HSCs and initiate liver fibrosis by releasing profibrotic cytokines. Our study found that FFA treatment increased the mRNA levels of CTGF in HepG2, but this increase was reversed by rosiglitazone treatment (FFA *vs.* Control, P = 0.0024; Rosiglitazone *vs.* FFA, P = 0.0087) (Fig. 3J). Similarly, the expression of inflammation-related genes (IL-1β (FFA *vs.* Control, P = 0.0001; Rosiglitazone *vs.* FFA, P = 0.0006), IL-6 (FFA *vs.* Control, P < 0.0001; Rosiglitazone *vs.* FFA, P < 0.0001) and tumor necrosis factor-α (TNFα) (FFA *vs.* Control, P = 0.0057; Rosiglitazone *vs.* FFA, P = 0.0364)) was also increased following FFA treatment, and rosiglitazone reversed this increase (Fig. 3K - M). Overall, these findings suggest that activation of PPARγ can ameliorate NAFLD.

3.3 Activation of TGF-β/Smad signaling pathway in NAFLD

To investigate the potential molecular mechanisms through which PPARγ influences NAFLD, we focused on the TGF-β/Smad signaling pathway. This pathway, mediated by TGF-β, Smad2/3, and Smad7, plays a central role in fibrosis across multiple organs[23]. To better understand the interactions between PPARγ and the mediators of the TGF-β/Smad signaling pathway, we conducted a protein interaction analysis using the String database. The results revealed a strong interaction between PPARγ and the TGF-β/Smad signaling members (Fig. 4A). Additionally, we observed a significant increase in both mRNA and protein levels of TGF-β in the NAFLD group compared to the control group (P < 0.0001 and P = 0.0022, respectively) (Fig. 4B, C). Furthermore, there was a notable decrease in the expression of Smad7 protein in the NAFLD group (P = 0.0048) (Fig. 4D). Previous research has suggested that Smad7 prevents the activation of Smad2/3[24]. Therefore, we further evaluated the

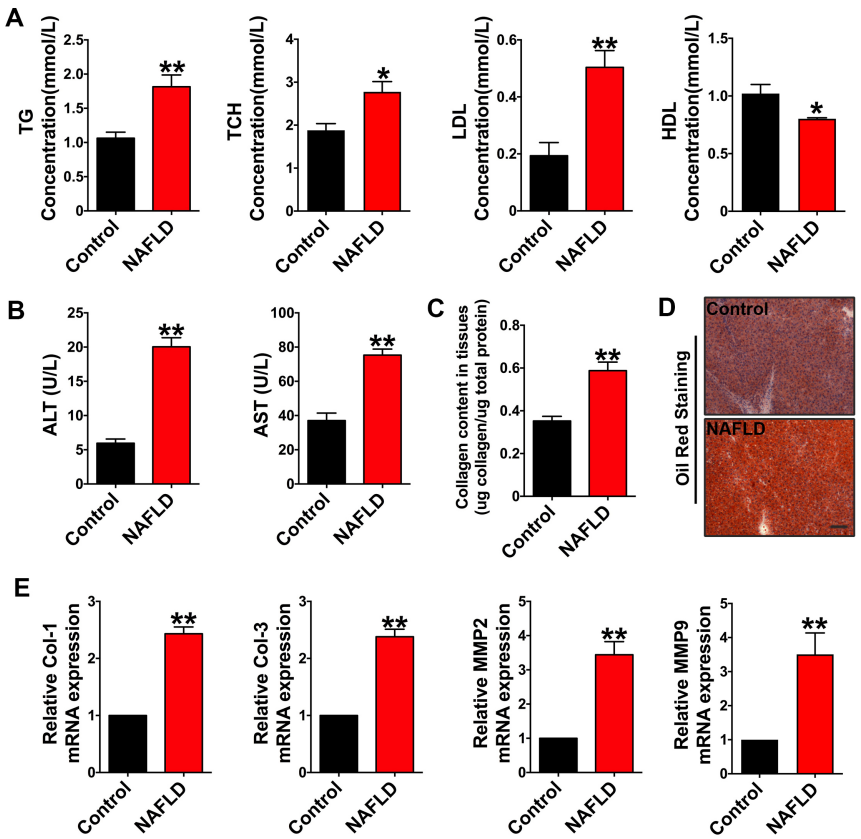

Fig. 1 Fibrosis and collagen deposition in a rat model of nonalcoholic fatty liver disease (NAFLD). (A) Triglycerides (TG), total cholesterol (TCH), low-density lipoprotein (LDL) and high-density lipoprotein (HDL) concentrations in the control and NAFLD groups. (N = 4-6), $^{*}P < 0.05$, $^{**}P < 0.01$, *vs.* Control. (B) The alanine aminotransferase (ALT) and aspartate aminotransferase (AST) levels in the control and NAFLD groups. (N = 5-6), $^{**}P < 0.01$, *vs.* Control. (C) Collagen contents in the liver homogenization samples, indicating collagen deposition in liver tissues in the control and NAFLD groups. (N = 3), $^{**}P < 0.01$, *vs.* Control. (D) Oil red O staining of tissue sections showing the lipid deposition in the liver. Scale bar indicates 200 μm. (N = 3). (E) type I collagens (Col-1), type III collagens (Col-3), matrix metalloproteinase 2 (MMP2), and matrix metalloproteinase 9 (MMP9) mRNA expression in the control and NAFLD groups. (N = 3-11), $^{**}P < 0.01$, *vs.* Control. Data are presented as means ± SEM.

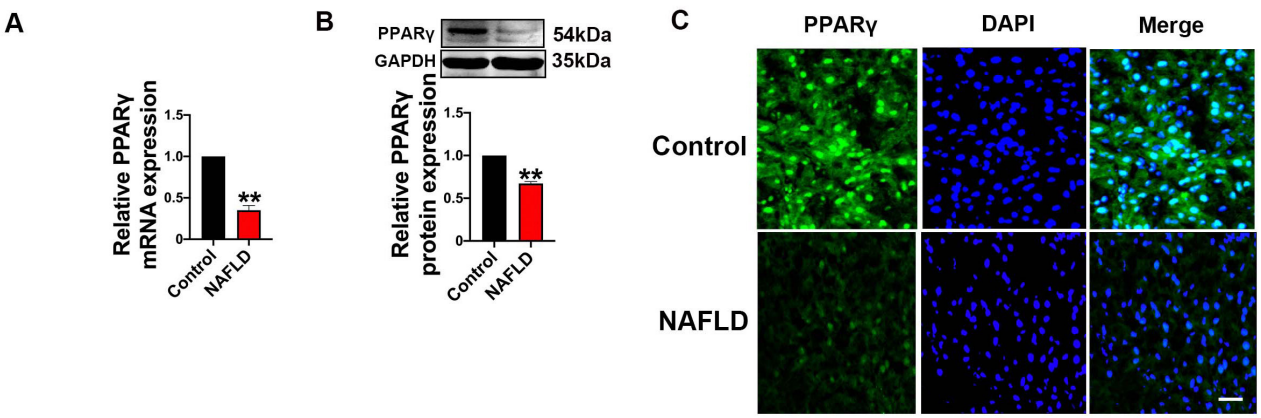

Fig. 2 The expression of peroxisome proliferator-activated receptor gamma (PPARγ) was decreased in nonalcoholic fatty liver disease (NAFLD). (A, B) Relative mRNA and protein levels of PPARγ in the control and NAFLD groups. (N = 9), $^{**}P < 0.01$, *vs.* Control. (C) Immunofluorescence results indicating the expression of PPARγ in the control and NAFLD groups. Scale bars: 100 μm.

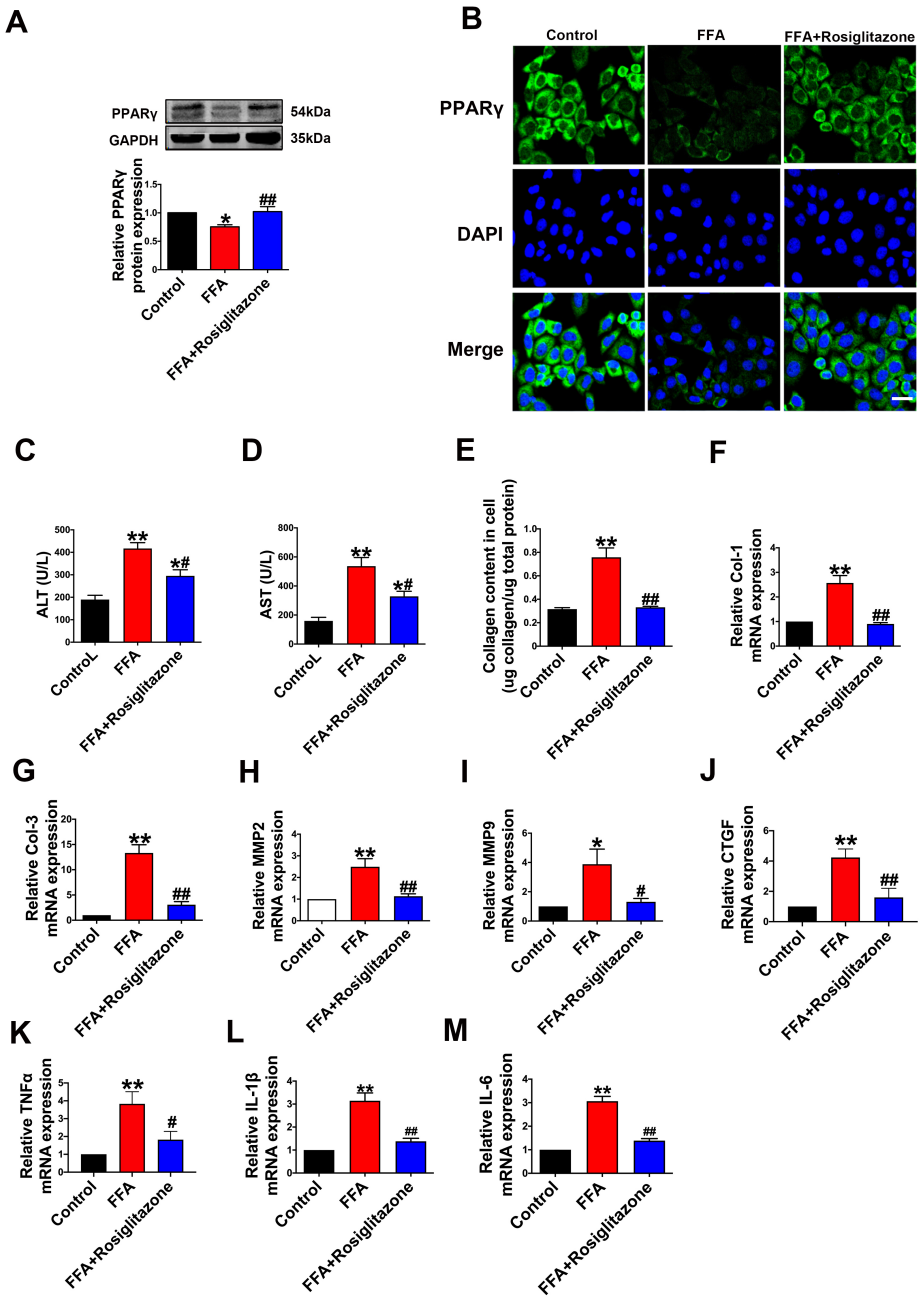

Fig. 3 Effect of peroxisome proliferator-activated receptor gamma (PPARγ) inhibition on hepatic fibrosis in nonalcoholic fatty liver disease (NAFLD). (A) Relative protein levels of PPARγ in the control, free fatty acid (FFA), and FFA+Rosiglitazone groups. ($N = 6$), $^{*}P < 0.05$, $^{**}P < 0.01$, *vs.* Control; $^{\#\#}P < 0.01$, *vs.* FFA. (B) Immunofluorescence results indicating the expression of PPARγ in the control, FFA, and FFA+Rosiglitazone groups. Scale bars: 50 μm. (C, D) ALT and AST concentrations in the control, FFA, and FFA+Rosiglitazone groups. ($N = 5$), $^{*}P < 0.05$, $^{**}P < 0.01$, *vs.* Control; $^{\#}P < 0.05$, *vs.* FFA. (E) Collagen contents in the control, FFA, and FFA+Rosiglitazone groups. ($N = 5$), $^{**}P < 0.01$, *vs.* Control; $^{\#\#}P < 0.01$, *vs.* FFA. (F-I) Col-1, Col-3, matrix metalloproteinase 2 (MMP2) and MMP9 mRNA levels in the control, FFA, and FFA+Rosiglitazone groups. ($N = 4$-5), $^{*}P < 0.05$, $^{**}P < 0.01$, *vs.* Control; $^{\#}P < 0.05$, $^{\#\#}P < 0.01$, *vs.* FFA. (J) The mRNA levels of connective tissue growth factor (CTGF) in the control, FFA, and FFA+Rosiglitazone groups. ($N = 4$), $^{**}P < 0.01$, *vs.* Control; $^{\#\#}P < 0.01$, *vs.* FFA. (K) Tumor necrosis factor-α (TNF-α) mRNA levels in the control, FFA, and FFA + Rosiglitazone groups. ($N = 4$), $^{**}P < 0.01$, *vs.* Control; $^{\#}P < 0.05$, *vs.* FFA. (L) Interleukin (IL)-1β mRNA level in the control, FFA, and FFA + Rosiglitazone groups. ($N = 4$), $^{**}P < 0.01$, *vs.* Control; $^{\#\#}P < 0.01$, *vs.* FFA. (M) The mRNA levels of IL-6 in the control, FFA, and FFA + Rosiglitazone groups. ($N = 4$), $^{**}P < 0.01$, *vs.* Control; $^{\#\#}P < 0.01$, *vs.* FFA. Data are presented as means ± SEM.

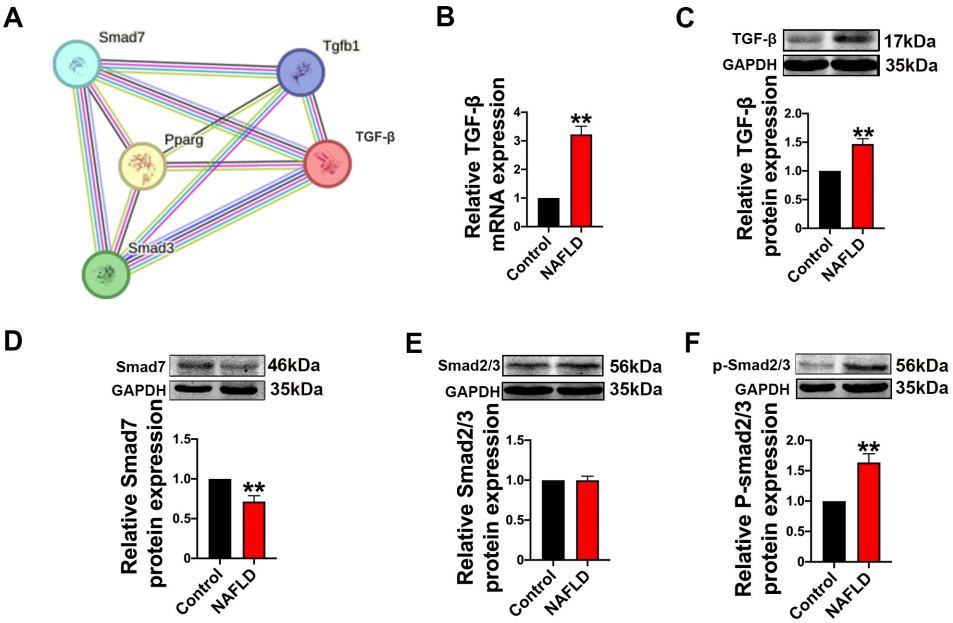

Fig. 4 Changes of the transforming growth factor (TGF)-β/Smad signaling pathway in nonalcoholic fatty liver disease (NAFLD). (A) Protein–protein interaction (PPI) network of peroxisome proliferator-activated receptor gamma (PPARγ), TGF-β, Smad2, Smad3, and Smad7 exported from STRING database (https: //string-db.org) (version 12.0). (B, C) Relative mRNA and protein levels of TGF-β in the control and NAFLD groups. ($N = 4$-5), $^{**}P < 0.01$, *vs.* Control. (D) Relative protein levels of smad7 in each group. ($N = 5$-8). $^{**}P < 0.01$, *vs.* Control. (E) Total smad2/3 protein levels in each group. ($N = 3$). (F) Phosphorylated protein levels of smad2/3 in each group. ($N = 10$), $^{**}P < 0.01$, *vs.* Control. Data are presented as means ± SEM.

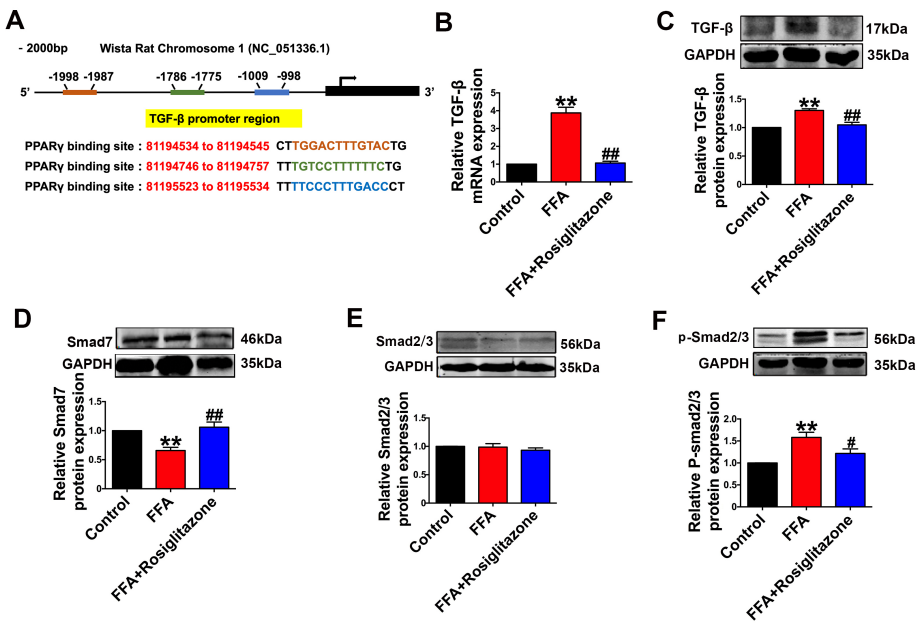

Fig. 5 Peroxisome proliferator-activated receptor gamma (PPARγ) inhibits the activation of the transforming growth factor (TGF)-β/Smad axis in nonalcoholic fatty liver disease (NAFLD). (A) PROMO database showing the sequences of the potential binding sites in the proximal region (2000 bp upstream) of TGF-β promoters. (B, C) Relative mRNA and protein levels of TGF-β in the control, free fatty acid (FFA), and FFA+Rosiglitazone groups. ($N = 4$-5), $^{**}P < 0.01$, *vs.* Control; $^{\#\#}P < 0.01$, *vs.* FFA. (D) Relative protein levels of Smad7 in the control, FFA, and FFA+Rosiglitazone groups. ($N = 4$), $^{**}P < 0.01$, *vs.* Control; $^{\#\#}P < 0.01$, *vs.* FFA. (E, F) Relative protein levels Smad2/3 and p-Smad2/3 expression in the control, FFA, and FFA+Rosiglitazone groups. ($N = 3$-4), $^{**}P < 0.01$, *vs.* Control; $^{\#}P < 0.05$, *vs.* FFA. Data are presented as means ± SEM.

expression of Smad2/3 in NAFLD group. As depicted in Fig. 4E, F, the levels of phosphorylated Smad2/3 proteins were significantly increased in the NAFLD group (P = 0.0003), while the expression of total Smad2/3 proteins remained unchanged. Based on these findings, we proposed a hypothesis that PPARγ may impact NAFLD by modulating the TGF-β/Smad signaling pathway.

3.4 Upregulation of PPARγ inhibited the activation of TGF-β/Smad signaling pathway in FFA-treated HepG2 Cells

Next, we examined whether PPARγ activation could affect TGF-β/Smad signaling activities. Analysis using the PROMO database revealed that the proximal regions of TGF-β promoters (2000 bp upstream) harbor the putative PPARγ binding sequences (Fig. 5A). We therefore examined the expression of TGF-β/Smad in three groups: Control, FFA, and FFA+Rosiglitazone. The results showed that rosiglitazone significantly decreased the expression of TGF-β in HepG2 cells compared to the FFA group (FFA *vs.* Control, P < 0.0001; Rosiglitazone *vs.* FFA, P < 0.001) (Fig. 5B, C). This decrease was accompanied by Smad7 up-regulation at the protein level (FFA *vs.* Control, P = 0.0081; Rosiglitazone *vs.* FFA, P = 0.003) (Fig. 5D). Additionally, rosiglitazone inhibited the expression of p-Smad2/3 in the presence of FFA (FFA *vs.* Control, P = 0.0034; Rosiglitazone *vs.* FFA, P = 0.0434), while the expression of total Smad2/3 remained unchanged in all groups (Fig. 5E, F).

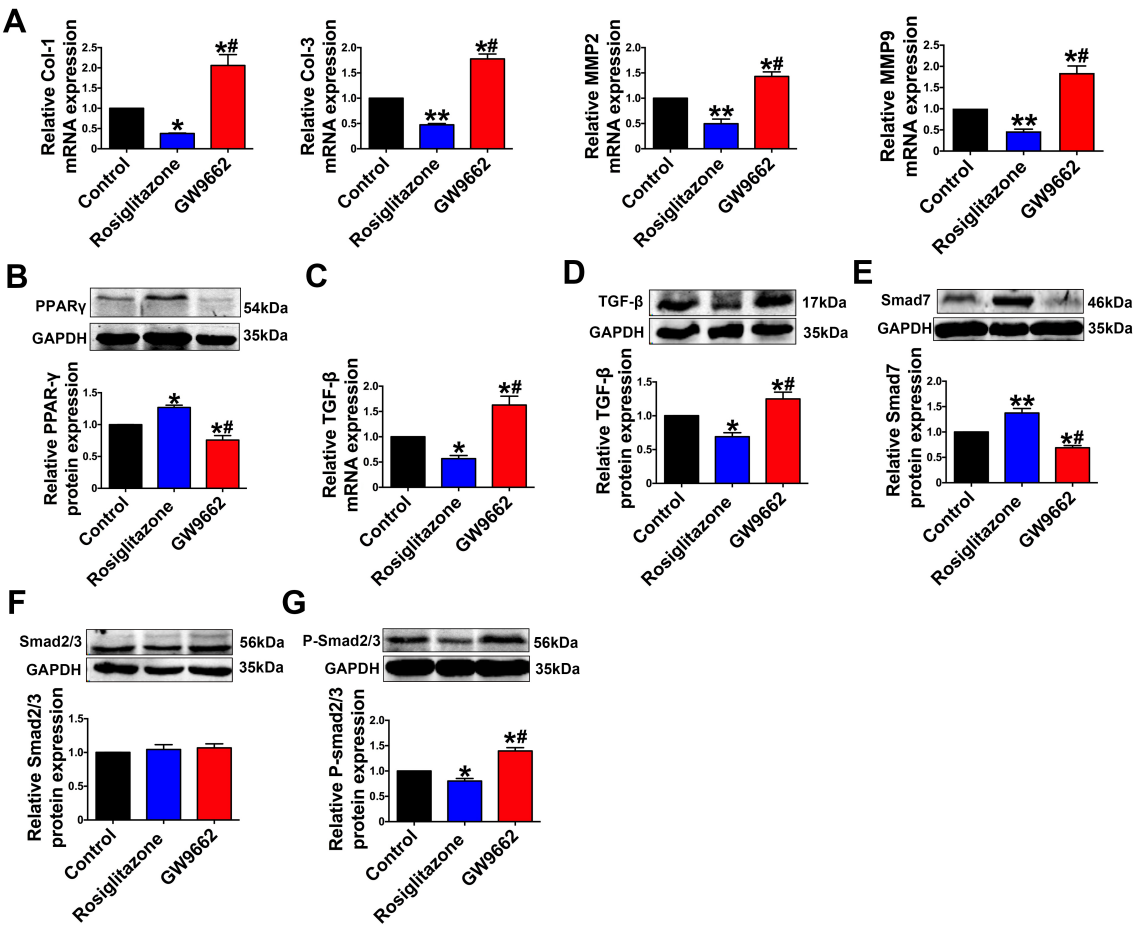

Fig. 6 Effect of peroxisome proliferator-activated receptor gamma (PPARγ) on the transforming growth factor (TGF)-β/Smad signaling pathway. (A) The mRNA expression levels of Col-1, Col-3, matrix metalloproteinase 2 (MMP2) and MMP9 in the control, rosiglitazone and GW9662 groups. (N = 3-5), $^{*}P$ < 0.05, $^{**}P$ < 0.01 *vs.* Control; $^{\#}P$ < 0.05, *vs.* Rosiglitazone. (B) The protein levels of PPARγ in the control, rosiglitazone, and GW9662 groups. (N = 3), $^{*}P$ < 0.05, *vs.* Control; $^{\#}P$ < 0.05, *vs.* Rosiglitazone. (C, D) Relative TGF-β mRNA and protein levels measured by real-time PCR and western blot analysis, respectively, in the control, rosiglitazone, and GW9662 groups. (N = 4-6), $^{*}P$ < 0.05, *vs.* Control; $^{\#}P$ < 0.05, *vs.* Rosiglitazone. (E) Relative protein levels of Smad7 in the control, rosiglitazone, and GW9662 groups. (N = 3), $^{*}P$ < 0.05, *vs.* Control; $^{\#}P$ < 0.05, *vs.* Rosiglitazone. (F) Total smad2/3 protein in the control, rosiglitazone and GW9662 groups. (N = 3). (G) Phosphorylation of smad2/3 in the control, rosiglitazone, and GW9662 groups. (N = 4), $^{*}P$ < 0.05, *vs.* Control; $^{\#}P$ < 0.05, *vs.* Rosiglitazone. Data are presented as means ± SEM.

3.5 PPARγ regulated hepatic fibrosis through TGF-β/Smad signaling pathway

To further investigate the impact of PPARγ on NAFLD and the role of TGF-β/Smad signaling pathway in this process, we conducted an experiment using HepG2 cells. The cells were treated with a PPARγ-specific agonist rosiglitazone (30μmol/L, 48 h) and a PPARγ-specific inhibitor GW9662 (30μmol/L, 48 h). Our results demonstrated that exposure to rosiglitazone reduced the mRNA levels of Col-1, Col-3, MMP2, and MMP9 (Rosiglitazone *vs.* Control, $P = 0.0466$, $P = 0.0015$, $P = 0.0025$, $P = 0.0069$, respectively), whereas GW9662 significantly increased their expression (GW9662 *vs.* Control, $P = 0.0024$, $P = 0.0002$, $P = 0.0068$, $P = 0.0002$, respectively) (Fig. 6A). Additionally, PPARγ protein levels were significantly elevated after treatment with rosiglitazone compared to the control group but decreased in the GW9662 group (Rosiglitazone *vs.* Control, $P = 0.0129$; GW9662 *vs.* Control, $P = 0.0209$) (Fig. 6B). Similarly, rosiglitazone treatment resulted in a significant decrease in TGF-β mRNA and protein levels, while TGF-β was elevated in the GW9662 group (Rosiglitazone *vs.* Control, $P < 0.05$; GW9662 *vs.* Control, $P < 0.05$) (Fig. 6C, D). In addition, Smad7 protein levels were increased by rosiglitazone but downregulated in the GW9662 group relative to other groups (Rosiglitazone *vs.* Control, $P = 0.0081$; GW9662 *vs.* Control, $P = 0.0193$) (Fig. 6E). Furthermore, we observed that p-Smad2/3 level was attenuated in the rosiglitazone group and increased significantly with GW9662 treatment (Rosiglitazone *vs.* Control, $P = 0.0403$; GW9662 *vs.* Control, $P = 0.0006$), while the expression of total Smad2/3 remained unchanged (Fig. 6F, G).

4 Discussion

In this study, we demonstrated, for the first time, that PPARγ activation attenuated collagen content and lipid deposition, thereby preventing the progression of hepatic fibrosis in NAFLD by targeting the TGF-β/Smad axis. The main findings of this study include: (1) Activation of PPARγ effectively inhibits collagen production and liver fibrosis in NAFLD. (2) The mechanism by which PPARγ regulates NAFLD is associated with changes in the activation of the TGF-β/Smad signaling pathway. Our study provides new insights into the functional activity of PPARγ in NAFLD and suggests the promising application of PPARγ in the prevention of hepatic fibrosis in NAFLD (Fig. 7).

PPARγ, a subtype of PPARs[25], is a crucial regulator of glucose and adipogenesis[26]. It is also known as an anti-fibrotic factor in the cardiovascular system. Additionally, previous studies have reported that PPARγ exhibits anti-inflammatory effects and plays a critical role in lipid homeostasis and insulin-resistant with activation by rosiglitazone and inhibition by GW9662[27-29]. NAFLD is characterized by a progressive decline in liver function attributed to lipid accumulation and inflammation, leading to marked distortion of liver architecture and loss of function. The molecular mechanisms underlying NAFLD are complex, with numerous substances implicated[30-31]. However, the role of PPARγ in regulating NAFLD remained unclear until our study. We found that the expression of PPARγ mRNA and protein was remarkably

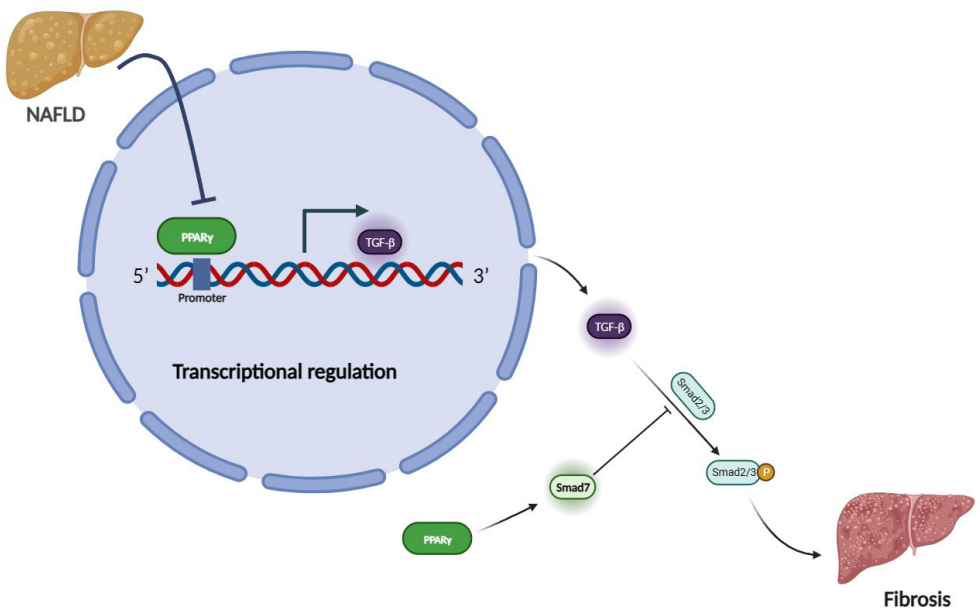

Fig. 7 Schematic diagram of the regulation of PPARγ on nonalcoholic fatty liver disease.

decreased in rat livers with NAFLD induced by HFD. Although various cell types in the liver can synthesize and secrete collagen, studies suggest that HSCs may play a leading role in collagen synthesis and secretion during hepatic fibrosis[8,32-33]. However, other research has demonstrated that hepatocytes increase their production of collagen during active fibrogenesis. majority of the newly synthesized hepatic collagen is produced by hepatocytes[34]. In this study, we used FFA to induce NAFLD model in HepG2 cells. Interestingly, we observed that FFA treatment increased fibrosis-related gene expression and collagen content in HepG2 cells. Activation of PPARγ restored the levels of Col-1, Col-3, MMP2, MMP9, and CTGF in HepG2 cells after FFA treatment and decreased mRNA levels of inflammation-related genes, suggesting an anti-inflammatory effect.

Our study proposed that PPARγ is directly related to hepatic fibrosis in NAFLD. Nevertheless, the underlying mechanisms by which PPARγ activation protects against hepatic fibrosis in NAFLD remain incompletely understood. TGF-β plays a crucial role in fibrosis by activating fibroblasts and producing collagen. We found that activation of TGF-β/Smad signaling was significantly increased *in vivo*. In addition, downregulation of PPARγ effectively increased TGF-β activation and aggravated NAFLD by promoting expression of fibrosis-related genes and collagen production in hepatocytes. Recently, plenty of studies suggested that TGF-β receptor activating resulted in Smad7 dissociated from the TGF-β receptor, and then phosphorylation of Smad2 and Smad3 are increased significantly[35-38]. Furthermore, we observed that PPARγ activation increased expression of Smad7 and decreased phosphorylation of Smad2 and Smad3 in HepG2 cells under FFA conditions, indicating regulation of hepatic fibrosis in NAFLD *via* the TGF-β/Smad pathway. These findings indicate that PPARγ activation exerts anti-NAFLD effects, including decreased ALT, AST, and collagen levels, particularly through suppression of the TGF-β/Smad axis and expression of fibrosis-related genes.

5 Conclusion

Our study identified, for the first time, that activation of PPARγ significantly improved the progression of NAFLD by inhibiting hepatic fibrosis. These findings provide compelling evidence that PPARγ exerts anti-fibrosis effects in NAFLD by modulating the TGF-β/Smad pathway. Consequently, PPARγ holds promise as an effective therapeutic agent for NAFLD.

Author contributions

Zhang Q W, Li J M and Zhang Y designed and conducted the experiments and wrote the manuscript. Zhu L W, Du M H, Zhao W J and Chen X M completed the design and operation of animal experiments. Zhang Q W, Dong X X and Zhang Z completed the molecular biology experiment. Hu Y Y and Sun Z Q performed the cell culture.

Source of funding

This research was funded by the National Natural Science Foundation of China (82273919 to Zhang Y) and the HMU Marshal Initiative Funding (HMUMIF-21022 to Zhang Y).

Ethical approval

Our animal experiments conformed to the recommendations of the Guide for the Care and Use of Laboratory Animals, published by the US National Institutes of Health (NIH Publication no. 85-23, revised 1996) and were approved by the ethics committee of Harbin Medical University (IRB3001722).

Conflicts of interests

Zhang Y is an Editorial Board Member of Frigid Zone Medicine. The article was subject to the journal's standard procedures, with peer review handled independently of this Member and his research groups.

Data availability statement

The data that support the findings of this study are available from the corresponding author upon reasonable request.

References

[1] Le M H, Le D M, Baez T C, *et al.* Global incidence of non-alcoholic fatty liver disease: A systematic review and meta-analysis of 63 studies and 1,201,807 persons. J Hepatol, 2023; 79(2): 287-295.
[2] Chen H, Zhan Y, Zhang J, *et al.* The global, regional, and national burden and trends of NAFLD in 204 Countries and territories: an analysis from global burden of disease 2019. JMIR Public Health Surveill, 2022; 8(12): e34809.
[3] Xia M, Sun X, Zheng L, *et al.* Regional difference in the susceptibility of non-alcoholic fatty liver disease in China. BMJ Open Diabetes Res Care, 2020; 8(1): e001311.

[4] Liu S, Liu Y, Wan B, *et al.* Association between vitamin D status and non-alcoholic fatty liver disease: a population-based study. J Nutr Sci Vitaminol (Tokyo), 2019; 65: 303-308.
[5] Jain R, Wade G, Ong I, *et al.* Determination of tissue contributions to the circulating lipid pool in cold exposure *via* systematic assessment of lipid profiles. J Lipid Res, 2022; 63(7): 100197.
[6] Su D, Zhou T, Wang Y, *et al.* Cold exposure regulates hepatic glycogen and lipid metabolism in newborn goats. Int J Mol Sci, 2023; 24(18): 14330.
[7] Heda R, Yazawa M, Shi M, *et al.* Non-alcoholic fatty liver and chronic kidney disease: Retrospect, introspect, and prospect. World J Gastroenterol, 2021; 27(17): 1864-1882.
[8] Wang S, Tang C, Zhao H, *et al.* Network pharmacological analysis and experimental validation of the mechanisms of action of Si-Ni-San against liver fibrosis. Front Pharmacol, 2021; 12: 656115.
[9] Wei M, Yan X, Xin X, *et al.* Hepatocyte-specific Smad4 deficiency alleviates liver fibrosis *via* the p38/p65 pathway. Int J Mol Sci, 2022; 23(19): 11696.
[10] Li Z, Wang Z, Dong F, *et al.* Germacrone attenuates hepatic stellate cells activation and liver fibrosis *via* regulating multiple signaling pathways. Front Pharmacol, 2021; 12: 745561.
[11] Yuan S, Wei C, Liu G, *et al.* Sorafenib attenuates liver fibrosis by triggering hepatic stellate cell ferroptosis *via* HIF-1alpha/SLC7A11 pathway. Cell Prolif, 2022; 55(1): e13158.
[12] Seo H Y, Lee S H, Han E, *et al.* Evogliptin directly inhibits inflammatory and fibrotic signaling in isolated liver cells. Int J Mol Sci, 2022; 23(19): 11636.
[13] Song Y, Wei J, Li R, *et al.* Tyrosine kinase receptor B attenuates liver fibrosis by inhibiting TGF-beta/SMAD signaling. Hepatology, 2023; 78(5): 1433-1447.
[14] Vallee A, Vallee J N, Lecarpentier Y. PPARgamma agonists: potential treatment for autism spectrum disorder by inhibiting the canonical WNT/beta-catenin pathway. Mol Psychiatry, 2019; 24(5): 643-652.
[15] Khan R S, Bril F, Cusi K, *et al.* Modulation of insulin resistance in nonalcoholic fatty liver disease. Hepatology, 2019; 70(2): 711-724.
[16] Trauner M, Fuchs C D. Novel therapeutic targets for cholestatic and fatty liver disease. Gut, 2022; 71(1): 194-209.
[17] Snyder H S, Sakaan S A, March K L, *et al.* Non-alcoholic fatty liver disease: a review of anti-diabetic pharmacologic therapies. J Clin Transl Hepatol, 2018; 6(2): 168-174.
[18] Chang E, Park C Y, Park S W. Role of thiazolidinediones, insulin sensitizers, in non-alcoholic fatty liver disease. J Diabetes Investig, 2013; 4(6): 517-524.
[19] Li J, Gong L, Zhang R, *et al.* Fibroblast growth factor 21 inhibited inflammation and fibrosis after myocardial infarction *via* EGR1. Eur J Pharmacol, 2021; 910: 174470.
[20] Zhang Q, Chen X, Hu Y, *et al.* BIRC5 inhibition is associated with pyroptotic cell death *via* Caspase3-GSDME pathway in lung adenocarcinoma cells. Int J Mol Sci, 2023; 24(19): 14663.
[21] Li J, Li Y, Liu Y, *et al.* Fibroblast growth factor 21 ameliorates Na(V)1.5 and Kir2.1 channel dysregulation in human AC16 cardiomyocytes. Front Pharmacol, 2021; 12: 715466.
[22] Li J, Xu C, Liu Y, *et al.* Fibroblast growth factor 21 inhibited ischemic arrhythmias *via* targeting miR-143/EGR1 axis. Basic Res Cardiol, 2020; 115(2): 9.
[23] Zhou Q Y, Yang H M, Liu J X, *et al.* MicroRNA-497 induced by Clonorchis sinensis enhances the TGF-beta/Smad signaling pathway to promote hepatic fibrosis by targeting Smad7. Parasit Vectors, 2021; 14(1): 472.
[24] Ganai A A, Husain M. Genistein attenuates D-GalN induced liver fibrosis/chronic liver damage in rats by blocking the TGF-beta/Smad signaling pathways. Chem Biol Interact, 2017; 261: 80-85.
[25] Porcuna J, Minguez-Martinez J and Ricote M. The PPARalpha and PPARgamma epigenetic landscape in cancer and immune and metabolic disorders. Int J Mol Sci, 2021; 22(19): 10573.
[26] Hendawy O, Gomaa H A M, Hussein S, *et al.* Cold-pressed raspberry seeds oil ameliorates high-fat diet triggered non-alcoholic fatty liver disease. Saudi Pharm J, 2021; 29(11): 1303-1313.
[27] Wu X, Cheng B, Guo X, *et al.* PPARalpha/gamma signaling pathways are involved in Chlamydia pneumoniae-induced foam cell formation *via* upregulation of SR-A1 and ACAT1 and downregulation of ABCA1/G1. Microb Pathog, 2021; 161(Pt B): 105284.
[28] Shan S, Zhou J, Yin R, *et al.* Millet bran protein hydrolysate displays the anti-non-alcoholic fatty liver disease effect *via* activating peroxisome proliferator-activated receptor gamma to restrain fatty acid uptake. J Agric Food Chem, 2023; 71(3): 1628-1642.
[29] He J, Hong B, Bian M, *et al.* Docosahexaenoic acid inhibits hepatic stellate cell activation to attenuate liver fibrosis in a PPARgamma-dependent manner. Int Immunopharmacol, 2019; 75: 105816.
[30] Fiorucci S, Distrutti E. Linking liver metabolic and vascular disease *via* bile acid signaling. Trends Mol Med, 2022; 28(1): 51-66.
[31] Kim E R, Park J S, Kim J H, *et al.* A GLP-1/GLP-2 receptor dual agonist to treat NASH: targeting the gut-liver axis and microbiome. Hepatology, 2022; 75(6): 1523-1538.
[32] Brougham-Cook A, Jain I, Kukla D A, *et al.* High throughput interrogation of human liver stellate cells reveals microenvironmental regulation of phenotype. Acta Biomater, 2022; 138: 240-253.
[33] Wu G, Liu Y, Feng W, *et al.* Hypoxia-induced adipose lipolysis requires fibroblast growth factor 21. Front Pharmacol, 2020; 11: 1279.
[34] Chojkier M, Lyche K D, Filip M. Increased production of collagen *in vivo* by hepatocytes and nonparenchymal cells in rats with carbon tetrachloride-induced hepatic fibrosis. Hepatology, 1988; 8(4): 808-814.
[35] Wehrhan F, Hyckel P, Guentsch A, *et al.* Bisphosphonate-associated osteonecrosis of the jaw is linked to suppressed TGFbeta1-signaling and increased Galectin-3 expression: a histological study on biopsies. J Transl Med, 2011; 9: 102.
[36] Hilt Z T, Maurya P, Tesoro L, *et al.* Beta2M signals monocytes through non-canonical TGFbeta receptor signal transduction. Circ Res, 2021; 128(5): 655-669.
[37] Zhong C, Lin Z, Ke L, *et al.* Recent research progress (2015-2021) and perspectives on the pharmacological effects and mechanisms of tanshinone IIA. Front Pharmacol, 2021; 12: 778847.
[38] Tian H, Liu H, Yu J, *et al.* PHF14 enhances DNA methylation of SMAD7 gene to promote TGF-beta-driven lung adenocarcinoma metastasis. Cell Discov, 2023; 9(1): 41.